Available online at www.sciencedirect.com
SCIENCE DIRECT®
Nonlinear Analysis 63 (2005) e2165–e2176
Nonlinear Analysis
www.elsevier.com/locate/na

Nonlinear strain models in the analysis of quantum dot molecules

R.V.N. Melnik[a,*], B. Lassen[a], L.C. Lew Yan Voon[b], M. Willatzen[a], C. Galeriu[b]

[a] *Mads Clausen Institute, University of Southern Denmark, Grundtvigs Alle 150, DK-6400 Sønderborg, Denmark*
[b] *Department of Physics, Worcester Polytechnic Institute, 100 Institute Road, Worcester, MA 01609, USA*

Abstract

Strain effects are fundamental to optoelectromechanical properties of low-dimensional semiconductor nanostructures such as quantum dots (QDs). Nevertheless, their influence is typically analyzed with simplified linear models based on the minimization of uncoupled, purely elastic energy functionals with respect to displacements. The applicability of such models is limited to the study of isolated idealized quantum dots, and both coupled and nonlinear effects need to be accounted for in the analysis of more realistic structures. In this paper, generalizations of the existing models for bandstructure calculations are discussed in the context of strain effects. Examplifications are given for hexagonal WZ semiconductor nanostructures.

Keywords: Quantum dots; Modeling; Coupled PDEs; Strain; Bandstructures

1. Introduction

For the last four decades, mathematical models for studying electronic properties of single charge carriers have been extensively utilized by scientists to study optical properties of semiconductor quantum structures. The interest to such models has increased even

* Corresponding author. Canada Research Chair in Mathematical Modelling, Laurier University, 75 University Avenue West, Waterloo, Ont., Canada N2L 3C5. Tel.: +1 318 257 3198; fax: +1 318 257 3823.
E-mail address: rmelnik@wlu.ca (R.V.N. Melnik).

0362-546X/$ - see front matter © 2005 Elsevier Ltd. All rights reserved.
doi:10.1016/j.na.2005.02.043

further with new technological advances in applications of low-dimensional semiconductor nanostructures (LDSN) where the motion of electrons can be confined spatially. Such quantum mechanical models, applied to bandstructure calculations, are usually based on a simple linear Schrodinger model in the steady-state approximation. This approximation provides a sound basis for modeling in a number of situations, in particular where the emphasis is made on basic understanding of physical processes. Recent experiments (e.g. [15]), however, have suggested that such a consideration may be too simplistic for modeling realistic objects based on LDSNs due to neglecting many effects that may influence profoundly optoelectromechanical properties of the nanostructures. One such effect is strain relaxation.

Recall that the formation of LDSNs, in particular quantum dots, is a competition between the surface energy in the structure and strain energy. Technologically, all effective methodologies are based on self-assembly where the final result is many (dozens and often hundreds) self-assembled dots sitting on the wetting layer and randomly distributed over it, having different size, shape, and, ultimately, properties. Strain effects in such structures may influence drastically on the overall nanostructure properties. These effects will become increasingly important for current and potential applications of LDSNs. In life sciences, quantum dots can be used as biological tags representing, for example, a viable alternative to organic fluorescence probes in cell biology and biomedicine. In quantum computing, quantum dots can be used for constructing quantum bits using a spin confined to them. Starting from applications in photodectors and laser-based emitters, the range of applicability of LDSNs continues to grow. In many of these applications, we need to collect the emitted light from the array of quantum dots which, from both technological and modeling points of view, will require dealing with additional strain on the nanostructure (due to the presence of an optical fiber tip, for example [5]).

In this paper, we review critically the existing models for studying electronic properties of low-dimensional nanostructures and discuss their generalizations in the context of strain effects. The discussion is centered around hexagonal WZ GaN/AlN quantum dots and arrays. In Section 2, we describe our main premises for modeling electronic properties of LDSNs in the hierarchy of existing models. Section 3 is devoted to discussion of geometric and materials nonlinearities that need to be accounted for in modeling realistic LDSNs. In Section 4, we discuss how to incorporate systematically piezoelectric effects in the model, and possible ways to simplify the resulting 3D model. The variational formulation of our generalized model is discussed in Section 5. Several representative examples of calculations for hexagonal WZ quantum dot arrays are presented in Section 6, followed by concluding remarks.

2. Models for bandstructure calculations for low-dimensional semiconductors

A typical self-assembled semiconductor quantum dot nanostructure is an array (or a molecule) of many individual quantum dots sitting on the same "substrate" known as the wetting layer [10]. Each such dot contains several hundred thousand atoms. To account for quantum effects accurately, it is possible to apply ab initio or atomistic methodologies, but then one should face a task of enormous computational complexity in solving a large-scale

many-body problem. On the other hand, taken each quantum dot in isolation would lead to a manageable task for modern supercomputers (20 million atom simulations have been recently reported in [12]). However, accounting for the wetting layer even in the individual quantum dot model would increase the computational complexity of the problem in several times. As a result, the entire problem in its generality would be hardly feasible from a practical, routine-based simulation, point of view. Moreover, in calculating atomic positions the definitions of atomic forces that enter the Hamiltonian in such large scale atomic simulations are approximate by nature and a number of important coupled effects, such as piezoelectric, remain frequently outside the scope of the analysis. To attack the problem in hand, one needs to resort to some averaging over atomic scales. Such averaging are usually achieved by various empirical tight-binding, pseudopotential, and $k \cdot p$ approximations. The latter is well suited for our present consideration due to the fact that the $k \cdot p$ theory represents the electronic structure in a continuum-like manner and is well suited for incorporating additional effects into the model such as strain and piezoelectric effects.

In what follows, we are focusing on hexagonal WZ materials not only because this problem is more mathematically challenging compared to ZB materials, but mainly because there is evidence to suggest (e.g. [3]) that strain and piezoelectric effects are substantially more pronounced in such structures as compared to cubic materials. A $k \cdot p$ approximation is based on the envelope function approximation and its accuracy depends on the choice of the functional space where the envelope function is considered. The basis functions that span such a space correspond to subbands within conduction and valence bands of the semiconductor material and, although the higher number of basis functions would lead to more accurate results, in practical applications this number typically ranges from 1 to 8. Ultimately, the choice of the number of subbands in the basis is a balance between the accuracy of the model and computational feasibility of its solution. In our case of the WZ materials, spin–orbit and crystal-field splitting are important, as are valence and conduction band mixing (due to a large band gap typical for these materials). Hence, we use 6 valence subbands and 2 conduction subbands (accounting for spin up and down situations) to achieve a sufficient accuracy. Then, the model can be written in the form of the following eigenvalue PDE problem to be solved with respect to eigenpair (Ψ, E):

$$H\Psi = E\Psi, \quad \Psi = (\psi_S^{\uparrow}, \psi_X^{\uparrow}, \psi_Y^{\uparrow}, \psi_Z^{\uparrow}, \psi_S^{\downarrow}, \psi_X^{\downarrow}, \psi_Y^{\downarrow}, \psi_Z^{\downarrow})^{\mathrm{T}}, \tag{1}$$

where, for example, $\psi_X^{\uparrow} \equiv (|X\rangle \mid \uparrow)$ denotes the wave function component that corresponds to the X Bloch function of the valence band with the spin function of the missing electron "up", the subindex "S" denotes the wave function component of the conduction band, etc. E is the electron/hole energy. The Hamiltonian in (1) is taken here in the form of $k \cdot p$ theory

$$H \equiv H^{(\alpha,\beta)}(\vec{r}) = -\frac{\hbar^2}{2m_0} \nabla_i \mathscr{H}_{ij}^{(\alpha,\beta)}(\vec{r}) \nabla_j, \tag{2}$$

where $\mathscr{H}$ is the energy functional (defined, e.g., by the standard Kohn–Luttinger Hamiltonian, or its Burt–Foreman correction, and representing the kinetic energy plus a nonuniform potential field and other effects contributing to the total potential energy of the system), $\hbar$

is the Planck constant, m_0 is the free electron mass, $\vec{r} = (x, y, z)$, and the Einstein notation is used for repeated summation over spatial coordinates. The superindeces (α, β) denote a basis for the wave function of the charge carrier, so that in our case it will lead to an 8×8 matrix Hamiltonian.

Given the assumptions made above, the more precisely we define $\mathscr{H}$ in model (1)–(2), the more accurately we will be able to describe optoelectronic properties of the nanosystem. As we have already pointed out, one of the key effects that will increase the accuracy of the model is strain. However, accounting for strain effects in this model is far from trivial primarily due to the fact that in doing so we are attempting to link a microscopic (quasi-atomistic) description of the system with the effects that are pronounced at a larger-than-atomistic scale level as a result of interacting atoms. As a consequence of such a link, complex multiscale interactions will necessarily require some *averaging procedures* to be incorporated into the model. Indeed, atomic displacements *collectively* induce strain in our finite structure and this happens at the stage of growing the quantum dot from the crystal substrate wetting layer. Such strains will remain in the structure. When such a LDSN is used, for example in optoelectronics applications, this fact leads to a modification of the bandstructures obtainable for idealized situations without accounting for strain effects.

3. Geometric and material nonlinearities in finite LDSNs

First attempts to include strain effects in models (1)–(2) are due to Pikus and Bir with further substantial contributions by Rashba and Sheka and others [2]. The Hamiltonian that includes these effects is known as the Rashba–Sheka–Pikus (RSP) Hamiltonian. Although the premises of the theory remain largely untouched, a number of important results have been achieved in adapting and extending the RSP Hamiltonian to suit specific applications under consideration. In particular, the RSP Hamiltonian for WZ materials has been recently derived in [11] and applied to calculating bandstructures in [3].

One of the major drawbacks of the current approaches to modeling-strained LDSNs discussed in the previous section lies with the fact that they are not able to resolve adequately physical effects at edges, corners, and interfaces, including strain nonhomogeneities. All current models for bandstructure calculations, we are aware of, are based on the original representation of [2] where strain is treated on the basis of infinitesimal theory with Cauchy relationships between strain and displacements. However, geometric irregularities of the LDSN may render this approximation to be inadequate. In order to model finite (initially stressed) LDSNs in finite strain, we have to consider a more general case. As initial coordinates x_i of a material particle after deformation becomes $\xi_i = x_i + u_i$, we can define the result of this deformation by *the variation* of deformation $\delta\varepsilon_{ij}$ which is induced by the variation in displacements δu_i. This leads naturally to a variational formulation of the problem which, by no means, implies linear relationships between strain and displacements locally. Indeed, as the LDSN is an initially stressed object that should be considered in finite strain, we have the following relationship between strain ε_{ij} and the displacement

gradients $\partial u_i/\partial x_j$:

$$\varepsilon_{ij} = e_{ij} + \tfrac{1}{2}(e_{il}\omega_{lj} + e_{jl}\omega_{li}) + \tfrac{1}{2}\omega_{il}\omega_{jl}, \tag{3}$$

where $e_{ij} = (\partial u_i/\partial x_j + \partial u_j/\partial x_i)/2$ and $\omega_{ij} = (\partial u_i/\partial x_j - \partial u_j/\partial x_i)/2$ are translational (symmetric) and rotational (skew-symmetric) strain components, respectively, and l is the dummy summation index. This can be simplified in several different ways, depending on a practical situation. If we keep the above expressions in the second order terms only, we arrive at the standard Eulerian components of the strain which differ from the infinitesimal Cauchy representations by accounting for the quadratic terms

$$\varepsilon_{ij} = \frac{1}{2}\left(\partial u_i/\partial x_j + \partial u_j/\partial x_i + \frac{\partial u_k}{\partial x_i}\frac{\partial u_k}{\partial x_j}\right), \tag{4}$$

where the Einstein notation is used for summation. The above nonlinearities are of geometric origin and, formally, are due to the presence in (3) the rotational skew-symmetric operator. These nonlinearities should allow to account more accurately for strain inhomogeneities which, as it was pointed out recently in [8], may influence substantially on the nanosystem properties.

The other type of nonlinearity that should be mentioned in the context of modeling LDSNs is related to material nonlinearities expressed mathematically by stress–strain relationships. Since strain remains of orders of magnitudes smaller of the elastic limits, the linear relationship between stress and strain is a reasonable assumption at a first approximation. However, semiconductors are piezoelectrics and higher order effects may become important at the level of device simulation. At a more fundamental level, elastic and dielectric coefficients, being functions of the structure geometry, are nonlinear (leading ultimately to nonlinear stress–strain relationships), and one has to look critically at the valence-force-field approaches we use to treat elasticity. The standard Keating model (which has parameters that are unit-cell-dimension dependent) may not be sufficient and many body interactions of higher orders may need to be considered to account for anharmonicity effects and asymmetry of the interatomic potential. In this case, any reduction of the 3D models to models of lower dimensions (e.g., to two-dimensional models, for example, in cases of axial symmetry) should lead to nonlinear strain models.

4. Piezoelectric effects in bandstructure models and 3D reductions

Semiconductors are piezoelectric materials and the piezoelectric effect contributions cannot be ignored in bandstructure calculations, in particular for hexagonal WZ semiconductors. To find out equilibrium conditions for such materials, we need to solve a coupled system of three partial differential equations:

$$\frac{\partial \sigma_{ij}}{\partial x_j} + \rho F_i(\xi_l) = 0 \tag{5}$$

with appropriate boundary conditions (typically, we embed the LDSN in a larger matrix material where we assume Dirichlet boundary conditions for displacements). In (5), F_i are

components of structure (as a solid-state body) forces, taken at displaced points ξ_l, ρ is the density of the material, and σ_{ij} are the stress tensor components in index notation. The coordinate subindeces (Timoshenko–Karman notations) are obtained by changing $1 \to x, 2 \to y, z \to 3$ in the above tensorial representation, and for hexagonal WZ materials of interest corresponding components of the stress tensor have the form

$$\sigma_{xx} = c_{11}\varepsilon_{xx} + c_{12}\varepsilon_{yy} + c_{13}\varepsilon_{zz} - e_{13}E_z, \quad \sigma_{yy} = c_{12}\varepsilon_{xx} + c_{11}\varepsilon_{yy} + c_{13}\varepsilon_{zz} - e_{31}E_z,$$
$$\sigma_{zz} = c_{13}(\varepsilon_{xx} + \varepsilon_{yy}) + c_{33}\varepsilon_{zz} - e_{33}E_z, \quad \sigma_{yz} = c_{44}\varepsilon_{yz} - e_{15}E_y,$$
$$\sigma_{zx} = c_{44}\varepsilon_{zx} - e_{15}E_x, \quad \sigma_{xy} = \tfrac{1}{2}(c_{11} - c_{12})\varepsilon_{xy}. \tag{6}$$

Given (4), these are nonlinear relationships connecting the stress to the deformation gradient and the (piezo)electric field. The latter requires the Maxwell equation for the piezoelectric potential (assuming the external charge distribution, including ionic and free charges, negligible)

$$\nabla \cdot \mathbf{D}(r) = 0 \tag{7}$$

which, in its turn, should be coupled to system (5) by corresponding constitutive relations for the electric displacement vector as a function of both strains and the electric field, in addition to its dependency on nonlinear effects induced by spontaneous polarization. For the WZ hexagonal materials these relationships have the following form:

$$D_x = e_{15}\varepsilon_{zx} + \varepsilon_{11}E_x, \quad D_y = e_{15}\varepsilon_{yz} + \varepsilon_{11}E_y,$$
$$D_z = e_{31}(\varepsilon_{xx} + \varepsilon_{yy}) + e_{33}\varepsilon_{zz} + \varepsilon_{33}E_z + P_{\mathrm{sp}}, \tag{8}$$

where e_{ij} and ε_{ii} are piezoelectric and dielectric coefficients, respectively, and P_{sp} is the spontaneous polarization. The resulting system is solved with respect to (u_1, u_2, u_3, ϕ), where the potential is related to the electric field in the electrostatic manner $\mathbf{E} = -\nabla\varphi$. Note that electric enthalpy density $\bar{H}$ ($\mathbf{D} = -\nabla_{\mathrm{E}}\bar{H}$) is also a nonlinear function of both strain and the electric field (quadratic and cubic order terms are shown to be significant in a number of practical situations). Only first-order terms are accounted for in the present discussion.

A fact that has been overlooked in the literature on bandstructure calculations is that models like (5)–(8) are derived from a variational principle applied to the *total* potential energy which should include both deformational energy and piezoelectric field functionals [9]. Most results obtained so far in the context of bandstructure calculations are pertinent to minimization of elastic energy only (e.g. [1,3]). This may be an acceptable approximation for such materials as zinc-blende where the piezoelectric effect is relatively small. For WZ materials the minimization of the total potential energy is required. Formally, this requirement can be fulfilled by solving simultaneously Eqs. (5)–(8). If (4) are used, the resulting system is nonlinear. Note, however, that even in the linear approximation, the coupling between the field of deformation and the piezoelectric field is of fundamental importance. In a series of recent papers, Pan together with his collaborators has shown that at the device level the cost for neglecting coupling in strain calculations could lead to as high as a 30% error (e.g. [4] and references therein).

The type of geometric nonlinearities may differ depending on the type of the nanostructure we consider. In some cases, the general 3D model formulated above may be reduced. In particular, the effect of coupling between localized states in the wetting layer (as a possible

explanation for simultaneous excitations of multiple dots with different emission energies) can be studied with the von Karman "thin plate" model where we can account for both longitudinal and transverse deformations. The transverse shear terms in this case can be eliminated and we will be left with quadratic as the highest order terms:

$$\varepsilon_{xx} = \frac{\partial u_1}{\partial x} + \frac{1}{2}\left(\frac{\partial u_3}{\partial x}\right)^2, \quad \varepsilon_{yy} = \frac{\partial u_2}{\partial y} + \frac{1}{2}\left(\frac{\partial u_3}{\partial y}\right)^2,$$
$$\varepsilon_{xy} = \frac{1}{2}\left(\frac{\partial u_2}{\partial x} + \frac{\partial u_1}{\partial y} + \frac{\partial u_3}{\partial x}\frac{\partial u_3}{\partial y}\right). \tag{9}$$

This nonlinear model can be extended in a standard manner to include transverse shear (the nonlinear version of the Mindlin–Timoshenko model; see, e.g., [6]). For thin film nanorolls recently reported in the literature (e.g. [13]), the Flugge–Lurie–Byrne nonlinear thin shell model is an appropriate tool to apply.

In those cases where 3D bandstructure calculation models are amenable to dimensional reductions (e.g., [7,14]), the development of a reduction procedure depends on both material and geometrical parameters and in its generality represents a challenging task due to the presence of essentially 3D physical effects such as anisotropy, polarization, as well as of geometric inhomogeneities. We will briefly return to this issue in Section 5 for cylindrically asymmetric LDSNs.

5. Variational formulations and coupling bandstructure and strain calculations

As models described in Sections 2–4 are dealing with averaged atomic scales, all our Eqs. (1), (5), and (7) originate from variational formulations. While on the atomic scale we are attempting to move directly to new atomic positions of all particles after deformations (still under a series of assumptions), in our approach we move from the variation in displacements to the variation of deformation. In particular, the model we formulated in Section 4 is a consequence of the Hamilton principle:

$$\delta \int_{t_1}^{t_2} (L_0 + W)\,\mathrm{d}t = 0, \tag{10}$$

where L_0 is the Lagrangian of our LDSN, W represents contributions to the system behavior from body and surface forces, and t_1 and t_2 are two arbitrary moments of time such that $t_1 < t_2$. The Lagrangian of the nanostructure, considered as a solid-state object occupying volume V, including surface force and charge contributions, is

$$L = \int_V \left[\frac{1}{2}(\sigma^{\mathrm{T}}\varepsilon + E^{\mathrm{T}}D) - \rho\dot{u}^{\mathrm{T}}\delta\dot{u}\right] + \int_{S_\sigma} \bar{F}_1^{\mathrm{T}} u\,\mathrm{d}s + \int_{S_\varphi} \bar{F}_2^{\mathrm{T}}\varphi\,\mathrm{d}s, \tag{11}$$

where $\bar{F}_1$ and $\bar{F}_2$ are surface force and surface charge (with surface areas, S_σ and S_φ), respectively. Since the structure is embedded in a larger matrix configuration $\tilde{V}$, both $\bar{F}_1$ and $\bar{F}_2$ are assumed to be zero. Lagrangian (11) includes both the kinetic and potential energy contributions (elastic deformation and the energy of electric field). The associated model (1)–(2) for bandstructure calculations is static and hence we limit ourselves to the

steady-state solution of (10) which is found from the following variational formulation (see also [9]):

$$\int_{\tilde{V}} [-\sigma^{\mathrm{T}}(\delta\varepsilon_{\mathrm{L}} + \delta\varepsilon_{\mathrm{N}}) + D\delta E]\,\mathrm{d}v = 0. \tag{12}$$

Both piezoelectric stresses and the nonlinear part of the strain ε_{N} ($\delta\varepsilon = \delta\varepsilon_{\mathrm{L}} + \delta\varepsilon_{\mathrm{N}}$) are taken into account in the above formulation in a coupled consistent manner. As the formation of LDSNs is a competition between the surface energy in the structure and strain energy, the dynamics of the process may not always be ignored. In its essence, the problem is a free boundary value problem with the surface (interface) free energy defined as a nonlinear function of strain. The form of such a free energy functional was first derived by Marchenko and Parshin in the early 1980s. More recently, it has been shown (e.g., [8]) that substantial variations in stresses may be observed (in particular at surfaces and interfaces) on scales of order just a few atomic distances. Although, this makes a good argument for a complete large scale atomistic simulations of nanostructures, accounting for space–time scale interactions in such a case is infeasible at present, not only on any realistic time scale, but also for any realistic morphologies of quantum dot arrays.

Model (12) is coupled to the weak form of the Schrodinger equation which can be viewed as the problem of finding stationarity conditions for the following functional:

$$\Phi(\Psi) = -\frac{\hbar^2}{2m_0}\int_{\tilde{V}} (\nabla\Psi)^{\mathrm{T}}\mathscr{H}^{(\alpha,\beta)}\nabla\Psi\,\mathrm{d}v - E\int_{\tilde{V}} \Psi^{\mathrm{T}}\Psi\,\mathrm{d}v \tag{13}$$

with respect to the wave function vector field Ψ defined in (1). Under appropriate smoothness assumptions, such conditions lead to model (1), which from a mathematical point of view is the Euler–Lagrange equation associated with functional (13).

Our final remarks in this section go to the structure of the Hamiltonian under consideration. Formally, our Hamiltonian can be represented as a sum of constant and k-dependent energies:

$$H = H_0 + \tilde{\mathscr{H}}, \quad \tilde{\mathscr{H}} = H_1 + H_2 + H_3, \tag{14}$$

where H_0 (which is usually derived from the standard Kane Hamiltonian at $k = 0$) accounts for the spin-splitting effects. For the corresponding spin–orbit coupling matrix for the WZ materials see, e.g., [3,11]. The associated (with $k = 0$) matrix elements for the conduction band in (14) are zero. The second term, $\tilde{\mathscr{H}}$, consists of contributions of (a) the kinetic part of the microscopic Hamiltonian unit cell averaged by the respective Bloch function (S, X, Y, or Z), denoted as H_1 (b) the strain-dependent part of the Hamiltonian, denoted as H_2, and (c) the energy of unstrained conduction/valence band edges, denoted as H_3. For the conduction band, components of H_2 (the 1st and the 5th rows in the total Hamiltonian) are given as (e.g. [3])

$$H_2^{\mathrm{c}}(\vec{r}) = a_1\varepsilon_{zz} + a_2(\varepsilon_{xx} + \varepsilon_{yy}) \tag{15}$$

with the conduction band deformation potentials a_1 and a_2 (coordinate dependent, but constants within each material), while for the valence bands (the 2nd, 3rd, and 4th rows, respectively) we have

$$H_2^v(\vec{r}) = \begin{pmatrix} l_1\varepsilon_{xx} + m_1\varepsilon_{yy} + m_2\varepsilon_{zz} & n_1\varepsilon_{xy} & n_2\varepsilon_{xz} \\ n_1\varepsilon_{xy} & m_1\varepsilon_{xx} + l_1\varepsilon_{yy} + m_2\varepsilon_{zz} & n_2\varepsilon_{yz} \\ n_2\varepsilon_{xz} & n_2\varepsilon_{yz} & m_3(\varepsilon_{xx} + \varepsilon_{yy}) + l_2\varepsilon_{zz} \end{pmatrix}. \tag{16}$$

Representation (16) is given in the standard ($|X\rangle$, $|Y\rangle$, $|Z\rangle$) basis and the same expressions hold for the 6th, 7th, and 8th rows of our 8×8 Hamiltonian. In (16), l_i, m_j, and n_k are material specific characteristics defined in terms of the valence band deformation potentials (as before, coordinate-dependent, but constants within each material). Components of H_3 have diagonal entries of $-e\phi(\vec{r})$ where ϕ is the piezoelectric potential determined from (5)–(8) and e is the absolute value of the electron charge. H_1 has the standard form and for WZ materials can be found, for example, in [3]. Components of H_1 contain quadratic terms, related to the first-order differential operators, in such a way that the resulting system of 8 partial differential equations is of elliptic type.

In the case of cylindrical symmetry, it is desirable to reduce the general Hamiltonian for WZ structures, containing 10 parameters, to a simpler form. This can be done by applying the Sercel–Vahala (SV) approach to the RSP strain Hamiltonian (given for WZ structures, e.g., in [3,11]). The result is an extension of what has recently been reported in [7] to the hexagonal WZ materials. Based on such a reduced Hamiltonian, it is convenient to model rods, cylindrical nanowires and superlattices and we shall focus on modeling results obtained with this model elsewhere.

6. Interacting quantum dot molecules and their modeling

Theory described in the preceeding sections can also be applied directly not only to isolated, physically idealized quantum dots, but also to more realistic situations of quantum dot molecules. In what follows we present several representative examples of modeling five quantum dots embedded in a larger matrix. In order to compute optical spectra of such quantum dot arrays, first we solve four equilibrium equations (5), (7) with constitutive equations (6), (8) by using the finite element methodology. The outputs from this model allow us to define the Hamiltonian of system (2) on the same computational grid. By solving the remaining eight coupled elliptic PDEs (1), we find both eigenfunctions and energies corresponding to all subbands under consideration. In Fig. 1, we present strain distributions in the 5-dot quantum array, ε_{xy} and ε_{xz}. Piezoelectric potential in the array and the first "double" eigenstate in the conduction subband of the system is presented in Fig. 2. When analyzing eigenstates of this quantum dot molecule, we note that the lowest eigenvalue corresponds to a clearly localized state in a corner dot. Analyzing the next (in magnitude) eigenvalue, demonstrates a localized state at the diagonal from the first one. Next state will be localized in the center dot. The last one in this sequence will first exhibit "doubling" and that eigenstate is presented in the figure.

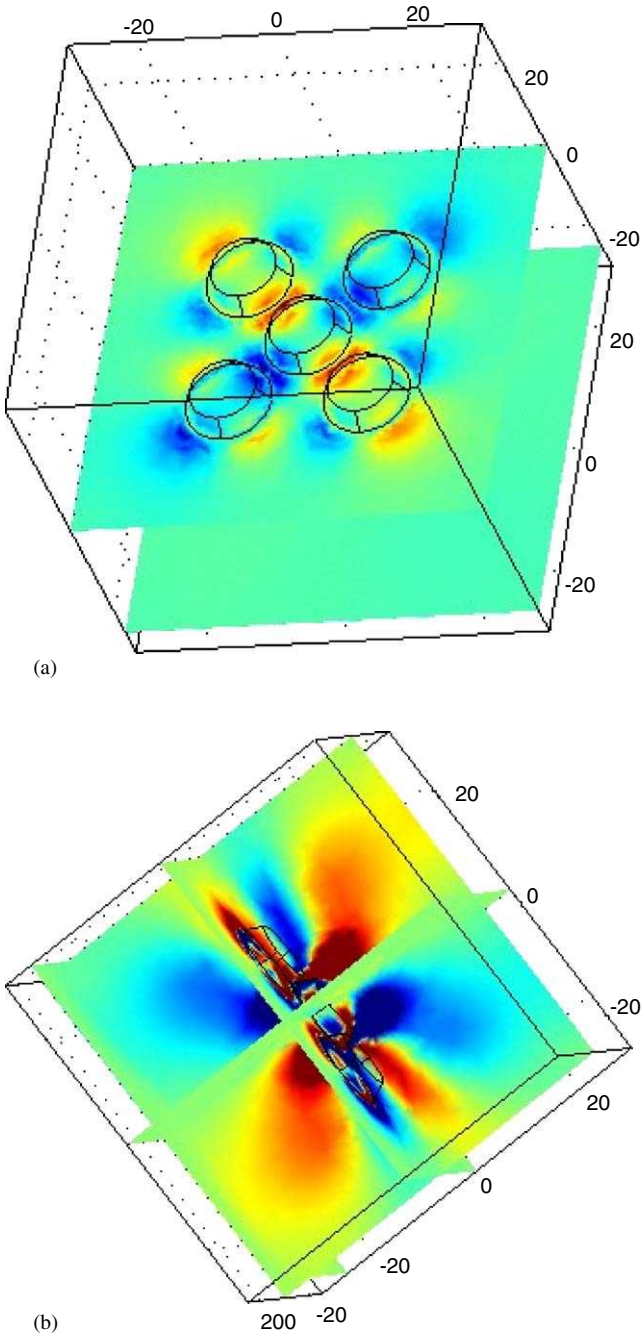

Fig. 1. Five-dot quantum dot molecule: strain distributions (ε_{xy}—left and ε_{xz}—right).

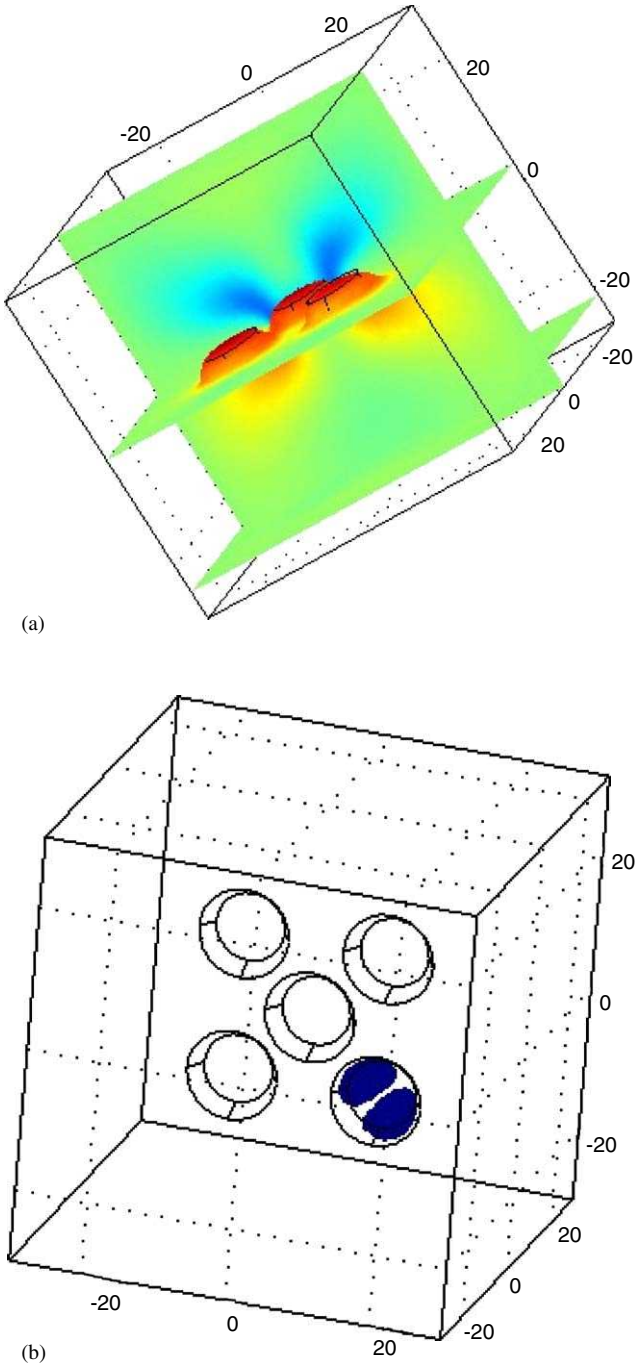

Fig. 2. Five-dot quantum dot molecule: piezoelectric potential (left) and the 6th eigenstate of the system (right).

The models reported here are also applicable to studying the interdot excitation transfer and spectral diffusion effects, observed experimentally with near-field scanning optical microscopy (e.g. [5]). As optical properties of dense quantum dot arrays differ substantially from those of low-density structures and isolated idealized quantum dots, these models should contribute further to study the effects of strain on bandstructures in such low-dimensional semiconductors.

References

[1] A.D. Andreev, E.P. O'Reilly, Theory of the electronic structure of GaN/AlN hexagonal quantum dots, Phys. Rev. B 62 (2000) 15851–15870.
[2] G.L. Bir, G.E. Pikus, Symmetry and Strain-Induced Effects in Semiconductors, Wiley, New York, 1974.
[3] V.A. Fonoberov, A.A. Balandin, Electronic properties of strained wurtzite and zinc-blende $GaN/Al_xGa_{1-x}N$ quantum dots, J. Appl. Phys. 94 (2003) 7178–7186.
[4] B. Jogai, J.D. Albrecht, E. Pan, Effect of electromechanical coupling on the strain in AlGaN/GaN HFETs, J. Appl. Phys. 94 (2003) 3984–3989.
[5] H.T. Johnson, R. Bose, Nonoindentation effect on the optical properties of self-assembled quantum dots, J. Mech. Phys. Solids 51 (2003) 2085–2104.
[6] J.E. Lagnese, J.-L. Lions, Modelling Analysis and Control of Thin Plates, Masson, Paris, 1990.
[7] L.C. Lew Yan Voon, R. Melnik, B. Lassen, M. Willatzen, Influence of aspect ratio on the lowest states of quantum rods, Nano Lett. 4 (2004) 289–292.
[8] M.A. Makeev, A. Madhukar, Large-scale atomistic simulations of atomic displacements, stresses, and strains in nanoscale mesas: effect of mesa edges, corners, and interfaces, Appl. Phys. Lett. 81 (2002) 3789–3791.
[9] R.V.N. Melnik, Generalised solutions, discrete models and energy estimates for a 2D problem of coupled field theory, Appl. Math. Comput. 107 (2000) 27–55.
[10] R.V.N. Melnik, M. Willatzen, Bandstructures of conical quantum dots with wetting layers, Nanotechnology 15 (2004) 1–8.
[11] F. Mireles, S.E. Ulloa, Strain and crystallographic orientation effects on the valence subbands of wirtzite quantum wells, Phys. Rev. B 62 (2000) 2562–2572.
[12] F. Oyafuso, G. Klimeck, P. von Allmen, T. Boykin, R.C. Bowen, Strain effects in large-scale atomistic quantum dot simulations, Phys. Stat. Solidi (b) 239 (2003) 71–79.
[13] O.G. Schmidt, K. Eberl, Thin solid films roll up into nanotubes, Nature 410 (2001) 168.
[14] M. Willatzen, R.V.N. Melnik, C. Galeriu, L.C. Lew Yan Voon, Quantum confinement phenomena in nanowire superlattice structures, Math. Comput. Simulation 65 (2004) 385–397.
[15] A. Zaslavsky, et al., Strain relaxation in silicon–germanium microstructures observed by resonant tunneling spectroscopy, Appl. Phys. Lett. 67 (1995) 3921.